

Chapter 10

Robinia Pseudoacacia and *Quercus Robur* Plantations Change the Physical Properties of *Calcic Chernozem*



Vadym Gorban

Abstract Steppe soils are assailed by various phenomena that diminish their fertility and degrade their physical properties. Afforestation is an effective way to arrest soil degradation. In the steppe zone of Ukraine, black locust (*Robinia pseudoacacia* L.) and pendunculate oak (*Quercus robur* L.) are most often planted but, in *Calcic chernozem*, plantations bring about changes in soil physical properties that are poorly understood. The most dramatic changes are observed in the A horizon: compared with soils under arable, the soil under woodland exhibits a lesser clay content and a greater content of silt and sand, a shift towards a greater proportion of larger water-stable aggregates, lesser particle density and greater total porosity.

Keywords Steppe soils · Forest plantings · Water-stable aggregates · Particle-size distribution · Total porosity

Introduction

Land degradation is an old adversary and, in most countries, still a current issue bringing significant changes that diminish soil fertility (Wunder and Bodle 2019; Jiang and others 2019; Banning and others 2008). In Ukraine, the most common soil degradation processes are a loss of organic matter and nutrients, compaction, acidification, waterlogging, and accelerated erosion by wind and runoff (Medvedev and others 2014). Afforestation arrests land degradation by protecting the soil surface from the elements, and by comprehensive improvement in various soil properties (Wiśniewski and Märker 2019; Gu and others 2019). Changes in the content of soil organic matter, nitrogen, carbon, and other chemical characteristics under woodland are well-described in the literature (amongst others Lal 2005; Foote and Grogan 2010; Clark and Johnson 2011; Jiao and others 2011) but changes in the physical properties of steppe soils have been neglected (Zhang and others 2017, 2018) so this study highlights the effects of plantings of black locust (*Robinia pseudoacacia* L.)

V. Gorban (✉)

Oles Honchar Dnipro National University, 72 Gagarin Avenue, Dnipro 49010, Ukraine
e-mail: vad01@ua.fm

and pendunculate oak (*Quercus robur* L.) on the complex of physical properties of *Calcic chernozem* (IUSS Working Group WRB 2015) in the Komissarovsky Forest Reserve in the central part of the steppe zone of Ukraine.

Materials and methods

Site characteristics

Figure 10.1 shows the location of the study area in the Komissarovsky Forest Reserve in Pyatikhatsky District of Dnepropetrovsk region. Site 1 (48°32'39.1"N 33°54'40.2"E) was located in an arable field that was bare at the time of sampling. Site 2 (48°31'52.8"N 33°54'07.1"E) was under a 50-year-old plantation of black locust: tree height 6-7 m, dbh 14-16 cm, spacing 0.6–0.7 m; the herbaceous ground cover was predominantly *Poa angustifolia*, *Chelidonium majus*, *Elytrigia repens* and *Geum urbanum*. Site 3 (48°31'52.4"N 33°54'29.9"E) was in a 70 year-old stand of oak: tree height 12-14 m, dbh 22-24 cm, spacing 0.8 m. *Acer campestre* was also present and the ground cover predominantly *Salvia verticillata*, *Ajuga genevensis*, *Verbascum lychnitis* and *Elytrigia repens*.



Fig. 10.1 Location of sites in the Komissarovsky Reserve

Sampling and laboratory procedures

In the summer of 2018, 2 kg composite soil samples were collected from each soil horizon to a depth of 1.5 m from each of the three plots. Samples were taken from the entire depth of each sampled layer. Particle-size distribution, aggregate-size distribution, size distribution of water-stable aggregates, bulk density, particle density and total porosity were determined in the laboratory following Carter and Gregorich (2006). Particle-size was determined by the pipette method, aggregate-size by dry sieving through a standard set of sieves of 10, 7, 5, 3, 2, 1, 0.5 and 0.25 mm mesh, size distribution of water-stable aggregates was determined by sieving in water and the results were expressed as a percentage of the mass of fractions of different sizes to the mass of the total soil sample. Dry bulk density (D_b) was measured on undisturbed 100cm³ samples collected using a drill; particle density (D_p) was determined using a pycnometer of volume 100cm³ and a 10 g soil sample; total porosity was calculated as $(1 - D_b/D_p) \times 100$.

Results

Under arable, the silt fraction predominates in all soil horizons (Table 10.1): the maximum silt and clay contents (62.2 and 35.0%, respectively) were observed in the Ck horizon, and the maximum sand content (8.8%) in the Bk horizon. The soil under both black locust and oak plantations also showed a greater silt content compared to other fractions; at the same time, there was a decrease in the sand content

Table 10.1 Particle-size distribution of *Calcic chernozem*

Horizon	Depth, m	Content of fraction, %		
		Sand	Silt	Clay
Site 1, arable				
A	0–0.5	6.4	59.7	33.9
Bk	0.5–0.8	8.8	59.1	32.1
Ck	0.8–1.5	2.8	62.2	35.0
Site 2, <i>R. pseudoacacia</i> plantation				
A	0–0.6	10.8	61.4	27.8
Bk	0.6–0.8	4.3	65.2	30.5
Ck	0.8–1.5	4.0	63.7	32.3
Site 3, <i>Q. robur</i> plantation				
A	0–0.7	12.4	62.4	25.2
Bk	0.7–0.9	4.0	63.1	32.9
Ck	0.9–1.5	5.0	63.7	31.3

and an increase in the silt and clay content with depth. Analysis of aggregate-size distribution revealed the strongest differentiation under arable with the 10–7 mm size the most common and its greatest content (27.4%) in the Ck horizon (Fig. 10.2a). The pattern is similar but less strongly expressed under the black locust plantation (Fig. 10.2b) with the predominant aggregate-size again being 10–7 mm but with the greatest content of this fraction in the Bk horizon (26.3%). Under the oak plantation (Fig. 10.2c), the aggregate-size fractions are evenly distributed across the size range with the maximum content of the 2–1 mm size fraction (17.3%) in the A horizon and the greatest content of the 10–7 mm in size fraction was in the Bk and Ck horizons.

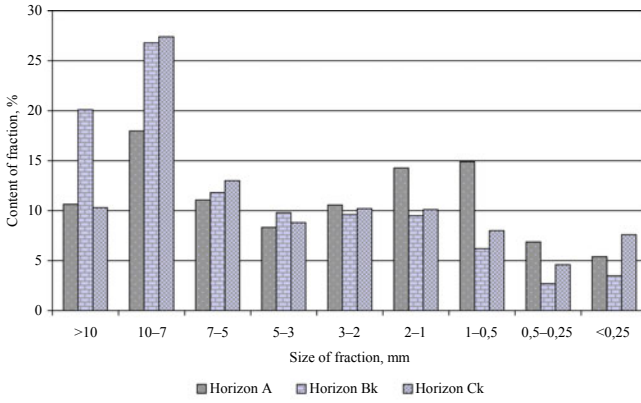
Table 10.2 presents the data for water-stable aggregates. Under arable, the most common aggregate size is < 0.25 mm which peaks in the A horizon (61.7%); the 0.5–0.25 mm fraction is also well represented. The picture is quite different under the woodland plantings: the least proportion of the < 0.25 mm fraction was in the A horizon, the greatest in the Ck horizon but in the A horizon and, to some extent in the Bk, there has been a significant shift towards larger water-stable aggregates, more especially under the longer-established oak plantation.

Table 10.3 presents data on bulk density, particle density and total pore space: under arable, the lowest bulk density (1.11 g/cm³) and lowest particle density (2.41/cm³) is in the A horizon in line with the visible concentration of soil organic matter and the maximum value of total porosity (53.1%) which decreases with depth. The A horizon under the black locust plantation also exhibits the lowest bulk density (1.12 g/cm³) and particle density and the greatest total pore space compared with the underlying Bk and Ck horizons. Under the older oak plantation, the A horizon exhibits yet lower bulk density (1.07 g/cm³) and particle density and even greater total pore space (55.2%) and this effect extends to the Bk horizon that shows a total porosity of 49.2%.

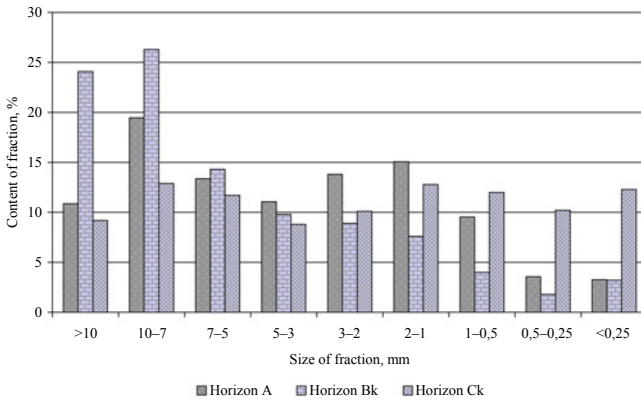
Discussion

Physical properties of the soil, such as particle-size distribution, bulk density and porosity, are interrelated. They have an important effect on both soil fertility (Zhang and others 2017) and on infiltration of rainfall, water holding capacity and transmissivity (Dent 2019), so research is relevant and necessary. Particle-size distribution affects almost every other soil attribute (Shangguan and others 2012); all horizons described here key out as silty clay loam (FAO 2006), except for the topsoil under the oak plantation which keys out as silt loam. The observed differences may well reflect chance textural variability between the sites (only three profiles have been analysed) and it is hard to account for the greater content of sand and silt and lesser content of clay in the topsoil under woodland plantations, as compared with adjacent arable, other than by deflation of the arable land and trapping of saltating sand grains by the woodland.

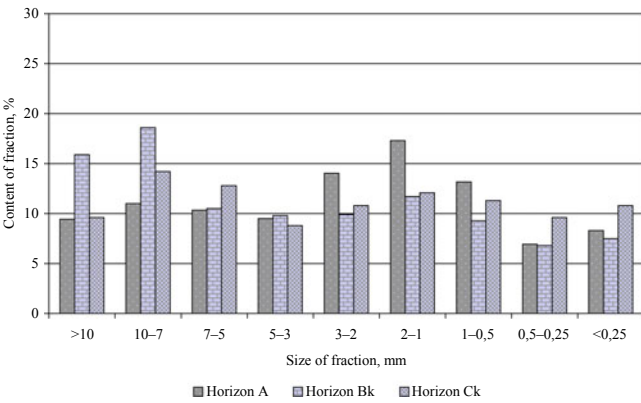
However, the contrasting aggregate-size distribution may well be an effect of the plantations, especially an increased content of the 3–2 mm and 2–1 mm size fractions



a



b



c

Fig. 10.2 Aggregate-size distribution of *Calcic chernozem*: a arable; b *R. pseudoacacia* plantation; c *Q. robur* plantation

Table 10.2 Size distribution of water-stable aggregates in *Calcic chernozem*

Horizon	Depth, m	Content of fraction (mm), %						
		> 5	5–3	3–2	2–1	1–0.5	0.5–0.25	< 0.25
Site 1—under arable								
A	0–0.5	0.2	0.3	0.9	2.1	8.2	26.5	61.7
Bk	0.5–0.8	0.1	0.8	2.1	9.5	15.4	20.5	51.6
Ck	0.8–1.5	0	0.4	0.9	3.0	10.7	28.5	56.5
Site 2—under <i>R. pseudoacacia</i> plantation								
A	0–0.6	3.5	3.0	4.6	11.9	26.1	19.2	31.8
Bk	0.6–0.8	0	0.2	1.5	6.7	20.3	34.4	36.9
Ck	0.8–1.5	0	0.4	0.6	1.9	9.0	28.0	60.1
Site 3—under <i>Q. robur</i> plantation								
A	0–0.7	2.4	3.8	10.7	18.6	17.3	15.9	31.3
Bk	0.7–0.9	0.1	0.4	1.0	4.1	12.4	29.7	52.3
Ck	0.9–1.5	0	0.3	0.4	2.0	8.0	26.4	62.9

Table 10.3 *Calcic chernozem*: bulk density, particle density and total pore space

Horizon	Depth, m	Bulk density, g/cm ³	Particle density, g/cm ³	Total porosity, %
Site 1—arable				
A	0–0.5	1.11	2.41	53.1
Bk	0.5–0.8	1.28	2.45	47.8
Ck	0.8–1.5	1.35	2.49	45.8
Site 2— <i>R. pseudoacacia</i> plantation				
A	0–0.6	1.12	2.39	47.3
Bk	0.6–0.8	1.36	2.45	44.5
Ck	0.8–1.5	1.40	2.3	44.7
Site 3— <i>Q. robur</i> plantation				
A	0–0.7	1.07	2.39	55.2
Bk	0.7–0.9	1.27	2.50	49.2
Ck	0.9–1.5	1.36	2.52	46.0

in the A horizon; similar changes under *R. pseudoacacia* plantations were described by Wang and others (2019). The ratio of the sum of fractions > 10 mm and < 0.25 mm to the sum of fractions 10–0.25 mm indicates the optimal aggregate-size distribution; the greater the ratio, the better aggregate-size distribution and we find that the ratio has increased by 1.5 under the black locust plantation and by 2.8 under the oak plantation. Whether this difference is a species effect or an effect of duration of the woodland, we cannot tell.

In the A horizon, the change in the size distribution of water-stable of aggregates compared with arable land is significant in size fractions from > 5 mm down to 1–0.5 mm. This is most marked in the size fractions of 3–2 and 2–1 mm under the oak plantation, which is accompanied by a reduction in bulk density and an increase in total pore space. This represents a significant improvement in soil physical properties in a relatively short period under woodland; the results are consistent with those reported by Li and others (2012). Over the longer period of 150 years, Li and Shao (2006) note that woodland plantations leads to a decrease in soil density values and an increase of total porosity. We should expect this improvement to be reflected in a greater infiltration rate, better available water capacity and increased resilience against erosion. Already, the A horizon itself is thicker by 10–20 cm under the woodland plantations compared with the adjacent arable land; which brings us full circle.

Conclusions

- *R. pseudoacacia* and *Q. robur* plantations have a significant, measurable, beneficial effect on the complex of physical properties of *Calcic chernozem*. This is manifest most strongly in the A horizon.
- Compared with the sampled profile from arable land, the A horizons of the two profiles under forest plantations show a 4–6% higher content of sand and silt and a 5–8% lower content of clay, which may or may not be connected with the woodland plantations.
- We can be confident that the woodland plantations are responsible for an increase in the content of soil aggregates in the 1–2 mm and 2–3 mm size fractions, and a significant increase in the proportion of water-stable aggregates larger than 0.5 mm, especially those greater than 1 mm. The 70-year-old oak plantation has had a greater effect than the 50-year-old black locust plantation.
- Changes in bulk density, particle density and total porosity follow the same pattern: the 70-year-old oak plantation producing lower bulk density and particle density and greater total pore space in the A horizon, and these effects extend more strongly into the underlying Bk horizon, than under the 50-year-old black locust plantation.

Acknowledgements The presented work is part of the scientific research of the Dept of Geobotany, Soil Science and Ecology of the Oles Honchar Dnipro National University, which is devoted to establishing the influences of forest plantations on steppe soils.

References

- Banning, N.C., C.D. Grant, D.L. Jones, and D.V. Murphy. 2008. Recovery of soil organic matter, organic matter turnover and nitrogen cycling in a post-mining forest rehabilitation chronosequence. *Soil Biology and Biochemistry* 40 (8): 2021–2031. <https://doi.org/10.1016/j.soilbio.2008.04.010>.
- Carter, M.R., and E.G. Gregorich, eds. 2006. *Soil sampling and methods of analysis*, 2nd ed. Boca Raton FL: CRC Press. <https://doi.org/10.1201/9781420005271>.
- Clark, J.D., and A.H. Johnson. 2011. Carbon and nitrogen accumulation in post-agricultural forest soils of western New England. *Soil Science Society of America Journal* 75 (4): 1530–1542. <https://doi.org/10.2136/sssaj2010.0180>.
- Dent, D.L. 2019. A standard for soil health. *International Journal of Environmental Studies* 77 (4): 613–618. <https://doi.org/10.1080/00207233.2019.169020>.
- FAO. 2006. *Guidelines for soil description*, 4th ed. Rome: Food and Agriculture Organization of the United Nations.
- Foote, R.L., and P. Grogan. 2010. Soil carbon accumulation during temperate forest succession on abandoned low productivity agricultural lands. *Ecosystems* 13 (6): 795–812. <https://doi.org/10.1007/s10021-010-9355-0>.
- Gu, C., X. Mu, P. Gao, et al. 2019. Influence of vegetation restoration on soil physical properties in the Loess Plateau. *China. Journal of Soils and Sediments* 19 (2): 716–728. <https://doi.org/10.1007/s11368-018-2083-3>.
- IUSS Working Group WRB. 2015. *World Reference Base for Soil Resources 2014, update 2015. International soil classification system for naming soils and creating legends for soil maps*. World Soil Resources Report 106. Rome: Food and Agriculture Organization of the United Nations.
- Jiang, C., J. Liu, H. Zhang, et al. 2019. China's progress towards sustainable land degradation control: Insights from the northwest arid regions. *Ecological Engineering* 127: 75–87. <https://doi.org/10.1016/j.ecoleng.2018.11.014>.
- Jiao, F., Z.M. Wen, and S.S. An. 2011. Changes in soil properties across a chronosequence of vegetation restoration on the Loess Plateau of China. *CATENA* 86 (2): 110–116. <https://doi.org/10.1016/j.catena.2011.03.001>.
- Lal, R. 2005. Forest soils and carbon sequestration. *Forest Ecology and Management* 220 (1–3): 242–258. <https://doi.org/10.1016/j.foreco.2005.08.015>.
- Li, W., M. Yan, Z. Qingfeng, and J. Zhikaun. 2012. Effects of vegetation restoration on soil physical properties in the wind-water erosion region of the Northern Loess Plateau of China. *Clean - Soil, Air, Water* 40 (1): 7–15. <https://doi.org/10.1002/clen.201100367>.
- Li, Y.Y., and M.A. Shao. 2006. Change of soil physical properties under long-term natural vegetation restoration in the Loess Plateau of China. *Journal of Arid Environments* 64 (1): 77–96. <https://doi.org/10.1016/j.jaridenv.2005.04.005>.
- Medvedev, V.V., I.V. Plisko, and O.N. Bigun. 2014. Comparative characterization of the optimum and actual parameters of Ukrainian chernozems. *Eurasian Soil Science* 47 (10): 1044–1057. <https://doi.org/10.1134/S106422931410007X>.
- Shangguan, W., Y. Dai, B. Liu, et al. 2012. A soil particle-size distribution dataset for regional land and climate modelling in China. *Geoderma* 171–172: 85–91. <https://doi.org/10.1016/j.geoderma.2011.01.013>.
- Wang, B., X. Zhao, Y. Liu, et al. 2019. Using soil aggregate stability and erodibility to evaluate the sustainability of large-scale afforestation of *Robinia pseudoacacia* and *Caragana korshinskii* in the Loess Plateau. *Forest Ecology and Management* 450: 117491. <https://doi.org/10.1016/j.foreco.2019.117491>.
- Wiśniewski, P., and M. Märker. 2019. The role of soil-protecting forests in reducing soil erosion in young glacial landscapes of Northern-Central Poland. *Geoderma* 337: 1227–1235. <https://doi.org/10.1016/j.geoderma.2018.11.035>.

- Wunder, S., and R. Bodle. 2019. Achieving land degradation neutrality in Germany: Implementation process and design of a land use change based indicator. *Environmental Science and Policy* 92: 46–55. <https://doi.org/10.1016/j.envsci.2018.09.022>.
- Zhang, X., J.F. Adamowski, R.C. Deo and others. 2018. Effects of afforestation on soil bulk density and pH in the Loess Plateau, China. *Water* 10 (12): 1710. Switzerland. <https://doi.org/10.3390/w10121710>.
- Zhang, X., Z. Yang, T. Zha, et al. 2017. Changes in the physical properties of soil in forestlands after 22 years under the influence of the conversion of cropland into farmland project in Loess region, Western Shanxi Province. *Shengtai Xuebao/Acta Ecologica Sinica* 37 (2): 416–424. <https://doi.org/10.5846/stxb201507291596>.